氢键桥连一维铁(Ⅲ)自旋交叉化合物的合成和性质

王康杰　李鸿庆　孙宇辰　王新益*

(南京大学化学化工学院，配位化学国家重点实验室，南京　210023)

摘要： 合成了一例单核铁(Ⅲ)化合物[Fe^{III}(Him)$_2$(4-MeOhapen)](CH$_3$SO$_3$) (**1**，Him=imidazole，H$_2$(4-MeOhapen)=N,N'-bis(4-methoxy-2-hydroxyacetophenylidene)ethylenediamine)，并对其晶体结构与磁性质进行了表征。单晶 X 射线分析表明，该化合物中的磺酸根阴离子通过氢键桥连[Fe^{III}(Him)$_2$(4-MeOhapen)]$^+$阳离子，并以此形成了一维链状结构。磁化率测试表明，该化合物具有突变型自旋交叉行为，其转变温度为 $T_{1/2}\downarrow$ =163 K 及 $T_{1/2}\uparrow$ =167 K。这些研究结果表明，阴阳离子之间的氢键对改进自旋交叉化合物的性质具有重要作用。

关键词： 三价铁配合物；自旋交叉；单晶结构；氢键

Synthesis and Properties of an Iron(Ⅲ) Spin Crossover Compound with 1D Chains Bridged by Hydrogen Bonds

WANG Kang-Jie　LI Hong-Qing　SUN Yu-Chen　WANG Xin-Yi*

(*State Key Laboratory of Coordination Chemistry, School of Chemistry and Chemical Engineering, Nanjing University, Nanjing* 210023, *China*)

Abstract: A mononuclear Fe(Ⅲ) compound [Fe^{III}(Him)$_2$(4-MeOhapen)](CH$_3$SO$_3$) (**1**, Him=imidazole, H$_2$(4-MeOhapen)= N,N'-bis(4-methoxy-2-hydroxyacetophenylidene)ethylenediamine) was synthesized and characterized structurally and magnetically. Single-crystal X-ray diffraction analysis revealed that the CH$_3$SO$_3^-$ anions bridge the [Fe^{III}(Him)$_2$(4-MeOhapen)]$^+$ cations by moderate hydrogen bonds to form one-dimensional chain structures. Magnetic susceptibility measurements revealed that compound **1** exhibits an abrupt spin crossover (SCO) with transition temperatures $T_{1/2}\downarrow$ =163 K and $T_{1/2}\uparrow$ =167 K. These results indicate that hydrogen bonds formed between the cationic and anionic centers play an important role in improving the SCO properties. CCDC: 1985363.

Keywords: Fe(Ⅲ) compound; spin crossover; single-crystal structure; hydrogen bond

0　Introduction

Recently, bistable materials with two switchable states in a certain range of external stimuli, including spin crossover (SCO) materials[1-2], single-molecule magnets (SMMs)[3-4], and organic radicals[5-6], have been extensively studied due to their potential applications on switches, sensors, memory devices and other fields[7]. Among them, the SCO compounds, usually octahedral Mn, Fe, and Co compounds with d^4 to d^7 electron configurations, can switch between high spin (HS) and low spin (LS) states in an external stimulus, such as temperature, light, and pressure. This change modifies their structure features and physical properties

including the magnetism, optics, conductivity and so on[1]. For more practical applications, researchers in the field are devoted to SCO compounds with wide thermal hysteresis loops at near room temperature[8].

Although Fe(II) SCO compounds have been studied the most by far, Fe(III) SCO compounds also have a broad prospect in future applications because of their higher air stability compared to the Fe(II) compounds[9-10]. Up to now, many hysteretic Fe(III) SCO compounds have been reported and the Fe(III) centers are coordinated by a wide variety of donor sets, including the N_4O_2, $N_2O_2S_2$, N_3O_2S and N_5O. For the organic ligands, most of the Fe(III) SCO compounds were synthesized using tridentate Schiff bases like Hqsal (Hqsal = N-(8-quinolyl)salicylaldimine) and its deriva-tives [9]. When it comes to tetradentate ligands, less than a dozen compounds have been reported and they are based on a salen-type N_2O_2 tetradentate ligand including salen, hapen, and acacen ligands (salen = N, N'-bis(salicylidene)ethylenediaminato, hapen = N, N'-bis(2-hydroxyacetophenylidene)ethylenediamine), and acacen = N, N'-bis(acetylacetone)ethylenediamine)[11-16]. Furthermore, although Matsumoto′s group has reported a series of [Fe^{III}(Him)$_2$(hapen)]Y·solvent compounds with different anions and solvents, few of them have distinct thermal hysteresis loops with transition temperature ($T_{1/2}$) higher than 100 K[11]. The design and even the control of the SCO behavior in these salen-type Fe(III) complexes are still challenging.

Hydrogen bond (H-bond) is one of the most important supramolecular interactions and is believed to be able to increase remarkably the cooperativity of the SCO compounds. With strong H-bonds, wide hysteresis loops are anticipated[5-6]. For example, Weber et al. reported in 2008 a Fe(II) SCO compound with a 70 K wide hysteresis loop at around room temperature. Strong H-bonds between the Fe(II) coordination spheres are responsible for the strong cooperativity in this compound[17]. Inspired by these considerations, our group has been interested in the design of SCO compounds where the H-bonds were introduced deliberately by using different organosulfonate anions, hoping to gain more control over their H-bonded

frameworks and SCO properties[18]. Our work confirmed that both the shapes and the sizes of the organodisul-fonates were correlated to the SCO properties, such as the transition temperatures and the abruptness of the transition[19].

Following these studies, we utilized the $CH_3SO_3^-$ as the counter anion in the [Fe^{III}(Him)$_2$(hapen)]$^+$ system, hoping to tune the property of this SCO system. Compared with the strong electron withdrawing -CF_3 group in $CF_3SO_3^-$, the electron donating -CH_3 group in $CH_3SO_3^-$ can increase the electron density in the O atoms of the anion, which might lead to stronger H-bonds with the imidazole (Him) molecules. We report here the synthesis and characterization of such a new Fe(III) compound, [Fe^{III}(Him)$_2$(4-MeOhapen)](CH_3SO_3) (**1**, H$_2$(4-MeOhapen) = N,N'-bis(4-methoxy-2-hydroxya-cetophenylidene) ethylenediamine), which is an SCO compound with a 4 K thermal hysteresis loop at above 160 K. Compared with the reported compound with the $CF_3SO_3^-$ anion[11], the different H-bond strength and bridging patterns should be responsible for the their different SCO properties.

1 Experimental

1.1 Reagents and physical measurements

All chemicals were purchased commercially and used without further purification. Elemental analyses for C, H, and N were measured on an Elementar Vario MICRO analyzer. Thermal Gravimetric Analysis (TGA) was measured in a Al_2O_3 crucible using a PerkinElmer TGA instrument in the temperature range of 20~700 ℃ under a N_2 flow at a heating rate of 20 ℃·min^{-1}. Magnetic measurement was measured under a dc field of 1 kOe with a Quantum Design VSM magnetometer. The experimental data were corrected for the diamag-netic contribution by means of Pascal′s constants.

1.2 Synthesis of [Fe^{III}(Him)$_2$(4-MeOhapen)] (CH_3SO_3) (1)

Compound **1** was prepared according to the synthetic procedure applied for compound [Fe(Him)$_2$(4-MeOhapen)]·PF$_6$[13]. The ligand H$_2$(4-MeOhapen) was prepared according to the general synthetic procedure of salen-type Schiff-base ligand. To a

solution of 4-methoxy-2-hydroxyacetophenone (0.1 mol, 16.62 g) in 50 mL of methanol was added a solution of ethylenediamine (0.05 mol, 3.01 g) in 50 mL of methanol. The mixture was stirred and refluxed for 30 min. After it was cooled to room temperature, yellow crystals precipitated. They were collected by suction filtration, washed with a small amount of methanol and diethyl ether, and dried *in vacuo*. The precursor Fe(Ⅲ) compound [FeCl(4-MeOhapen)]·H_2O was obtained as powders by mixing the ligand H_2(4-MeOhapen), iron(Ⅲ) chloride anhydrate, and trimethylamine in a 1:1:2 molar ratio in methanol. To a suspension of [FeCl(4-MeOhapen)]·H_2O (0.5 mmol, 0.22 g) in 10 mL of methanol, an excess of imidazole (5 mmol, 0.34 g) was added, and the mixture was stirred for 30 min on a hot-plate at 65 ℃. A solution of $Ag(CH_3SO_3)$ (0.5 mmol, 0.09 g) in 5 mL of methanol was added to the solution, and the resulting solution was stirred for 15 min before filtered. The filtrate was then added to a test tube, and diethyl ether vapor was allowed to diffuse into the test tube. Black block single crystals formed in the tube in 2 days. The crystals were then removed from the test tube and washed with a small amount of methanol. Yield: 0.21 g, 66%. Anal. Calcd. for $C_{27}H_{33}FeN_6O_7S$ (%): C, 50.55; H, 5.18; N, 13.10. Found (%): C, 50.91; H, 5.22; N, 12.54. IR (KBr, cm^{-1}): 3 132 (s), 3 051 (s), 3 014(s), 1 578(s), 1 531(s), 1 437(s), 1 240(s), 1 163(s), 1 028 (s), 841(s), 752(s), 619(s).

1.3　X-ray crystallographic study

Single crystal X-ray diffraction data were collected on a Bruker D8 Venture diffractometer with a CCD area detector (Ga $K\alpha$ radiation, λ=0.134 139 nm) at 190 K. The APEX Ⅲ program was used to determine the unit cell parameters and for data collection. The data were integrated and corrected for Lorentz and polarization effects using SAINT[20]. Absorption corrections were applied with SADABS[21]. The structure was solved by direct methods and refined by full-matrix least-squares method on F^2 using the SHELXTL crystallographic software package and OLEX 2[22-23]. All of the nonhydrogen atoms were refined anisotropically. Hydrogen atoms of the organic ligands were refined as riding on the corresponding non-hydrogen atoms. Additional details of the data collection and structural refinement parameters are provided in Table 1. The relevant coordination bond distances and angles are given in Table 2.

CCDC: 1985363.

Table 1　Crystal data and structure refinement for compound 1

Empirical formula	$C_{27}H_{33}FeN_6O_7S$	Z	2
Formula weight	641.5	D_c / (g·cm^{-3})	1.443
Temperature / K	190.06	μ / mm^{-1}	3.484
Crystal system	Triclinic	$F(000)$	670
Space group	$P\bar{1}$	Index ranges	$-11 \leqslant h \leqslant 11, -14 \leqslant k \leqslant 14, -16 \leqslant l \leqslant 15$
a / nm	0.972 15(4)	Reflection collected	13 519
b / nm	1.235 31(5)	Independent reflection	5 156 (R_{int}=0.067 7, R_σ=0.079 5)
c / nm	1.374 92(5)	Data, restraint, parameter	5 156, 0, 384
α / (°)	79.059(2)	Goodness-of-fit on F^2	1.1
β / (°)	72.768(2)	Final R indexes [$I \geqslant 2\sigma(I)$]	R_1=0.086 9, wR_2=0.249 3
γ / (°)	70.230(2)	Final R indexes (all data)	R_1=0.099 7, wR_2=0.262 7
V / nm^3	1.476 69(10)		

Table 2　Selected bond distances (nm) and bond angles (°) for compound 1

Fe(1)-N(1)	0.210 3(4)	Fe(1)-N(3)	0.214 9(4)	Fe(1)-O(1)	0.189 0(3)
Fe(1)-N(2)	0.210 5(4)	Fe(1)-N(5)	0.215 9(4)	Fe(1)-O(2)	0.189 1(3)
N(1)-Fe(1)-N(2)	81.97(15)	N(3)-Fe(1)-N(5)	174.47(15)	O(1)-Fe(1)-O(2)	100.51(14)

Continued Table 2
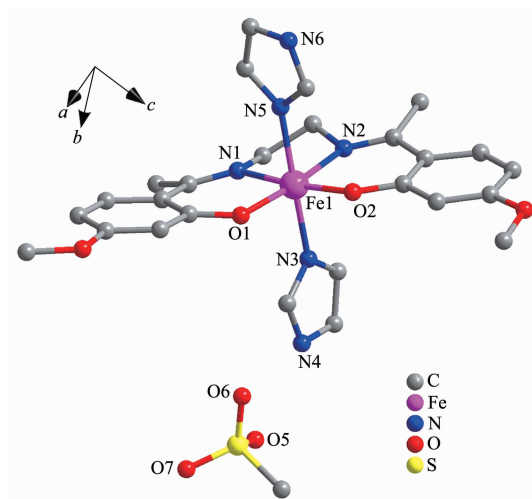
|					
N(1)-Fe(1)-N(3)	86.66(15)	O(1)-Fe(1)-N(1)	88.57(15)	O(2)-Fe(1)-N(1)	170.90(15)
N(1)-Fe(1)-N(5)	89.48(15)	O(1)-Fe(1)-N(2)	170.54(13)	O(2)-Fe(1)-N(2)	88.94(14)
N(2)-Fe(1)-N(3)	88.93(16)	O(1)-Fe(1)-N(3)	90.75(16)	O(2)-Fe(1)-N(3)	93.55(15)
N(2)-Fe(1)-N(5)	86.60(16)	O(1)-Fe(1)-N(5)	93.13(15)	O(2)-Fe(1)-N(5)	89.63(15)

2　Results and discussion

2.1　Description of the structure

Compound **1** crystallizes in a triclinic space group $P\bar{1}$. As we can see from its asymmetric unit shown in Fig.1, compound **1** has one crystallographic unique $[Fe^{III}(Him)_2(4\text{-MeOhapen})]^+$ cation and one $CH_3SO_3^-$ anion. The six-coordinated Fe(III) center adopts a distorted N_4O_2 octahedral geometry with the equatorial N_2O_2 donor atoms from the tetradentate 4-MeOhapen^{2-} ligand and two N atoms from two axial coordinated imidazole molecules. Regarding its SCO property, the Fe-N bond lengths (0.210 3(4)~0.215 9(4) nm) and O1-Fe1-O2 bond angle (100.51(14)°) at 190 K are both in the range of those reported for HS Fe(III) compounds with similar Schiff-base ligands[11-16], suggesting its HS state at 190 K. In addition, another structure parameter, namely the conformation of the five membered chelate ring involving ethylenediamine

moiety defined by Fe1, N1, C1, C2 and N2 atoms, is also related to its SCO property. As has been proposed by Murray et al., the envelope conformation allows the spin transition, and the gauche or planar conformation locks the metal center in high spin state[24]. For **1** at 190 K, the conformation of this FeC_2N_2 ring is indeed an envelope conformation, which will allow the SCO transition in **1**, as confirmed by the magnetic data below.

As designed, H-bonds are found in the structure between the imidazole molecules of the cationic motifs and the $CH_3SO_3^-$ anions. As shown in Fig.2, we can see that one-dimensional (1D) H-bond connected chains along the b axis are formed for **1**. Specifically, one $CH_3SO_3^-$ anion bridges two adjacent $[Fe^{III}(Him)_2(4\text{-MeOhapen})]^+$ cations by the N−H⋯O H-bonds between the O5 atom from the $CH_3SO_3^-$ anion and the N4-H4 and N6-H6 groups from the imidazole molecules. The details of these two H-bonds are listed in Table 3. We can see that these two H-bonds are of moderate strength with relatively short N⋯O distances (~0.28 nm). In addition, these 1D H-bonded chains are connected to each other with weak supramolecular interactions such as the weak N−H⋯π and C−H⋯π interactions with the N⋯π and C⋯π distances being

Fig.1　Asymmetric unit of molecule structure of **1**
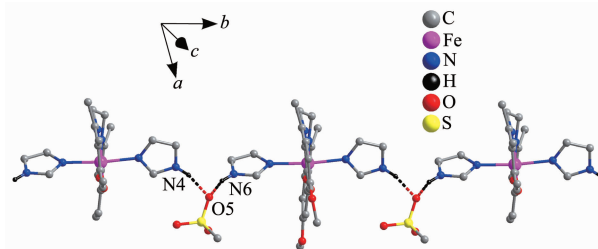
Fig.2　Hydrogen-bonded 1D structure of compound **1**

Table 3　Hydrogen bond parameters for compound 1

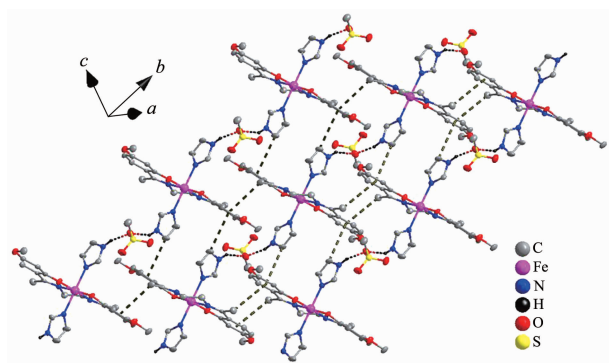| D−H⋯A	d(D⋯A) / nm	d(H⋯A) / nm	∠D−H⋯A / (°)
N(4)−H(4)⋯O(5)	0.279 70(69)	0.194 49(45)	162.709(312)
N(6)−H(6)⋯O(5)	0.280 87(58)	0.200 77(35)	150.669(331)

around 0.36 to 0.38 nm (Fig.3).

Fig.3　Weak N–H⋯π and C–H⋯π interchain
interactions in compound **1**

2.2　Thermal stability

　　To determine the thermal stability of compound **1**, its thermal behavior was investigated under nitrogen atmosphere by TGA. As shown in Fig.4, the TGA curve of compound **1** revealed that **1** was stable up to about 200 ℃. After that, it decomposed upon further heating. This result confirmed the stability of **1** and is consistent with the fact that there is no crystallized solvent molecule in **1**.
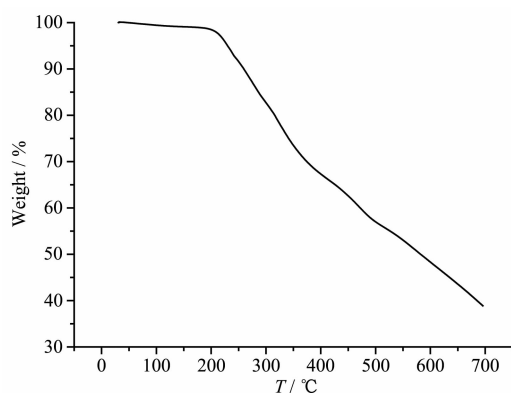

Fig.4　TGA curve of compound **1**

2.3　Magnetic property

　　Temperature dependent molar magnetic suscepti-bility data (χ_M) of **1** were measured on the grounded single crystals under an applied dc magnetic field of 1 000 Oe. The data were measured on lowering the temperature from 300 to 5 K at the first run and subsequently on elevating the temperature from 5 to 300 K at the second run with a temperature sweep rate of 5 K·min^{-1}. As can be seen from the plot of $\chi_M T$ versus T given in Fig.5, a complete abrupt spin

transition between the HS (S=5/2) and LS (S=1/2) states occurs for **1**. At 300 K, the $\chi_M T$ value was 4.60 cm^3·mol^{-1}·K, consistent with a HS Fe(Ⅲ) center with a g value of about 2.24[11,13]. Upon cooling, the $\chi_M T$ value remained nearly constant until 170 K, where it decreased abruptly to 1.30 cm^3·mol^{-1}·K at 130 K, and finally reached 1.04 cm^3·mol^{-1}·K at 5 K. The transition temperature was $T_{1/2}\downarrow$=163 K. The low temperature value was significantly larger than 0.375 cm^3·mol^{-1}·K for a spin-only LS value. This observation might be due to the residue HS Fe(Ⅲ) centers at low temperature and is similar to the reported Fe(Ⅲ) SCO comp-ounds[11,13]. Upon heating, similar $\chi_M T$ versus T curve was observed with a slightly higher transition temperature of $T_{1/2}\uparrow$=167 K. Therefore, compound **1** undergoes an abrupt SCO transition with a thermal hysteresis loop of 4 K width.
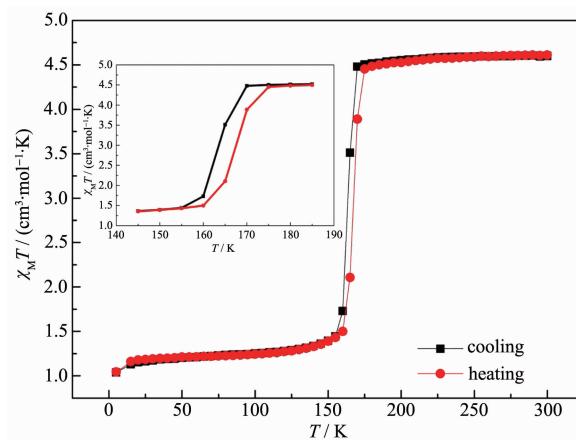
Inset: $\chi_M T$ vs T plots between 140 and 190 K showing hysteresis

Fig.5　Temperature dependent $\chi_M T$ plots for compound **1**
in the temperature region of 5 to 300 K

　　Although compound **1** has the same [Fe^{Ⅲ}(Him)$_2$(4-MeOhapen)]$^+$ cation with the reported [Fe^{Ⅲ}(Him)$_2$(4-MeOhapen)]·PF$_6$ and [Fe^{Ⅲ}(Him)$_2$(4-MeOhapen)]·CF$_3$SO$_3$ compounds, their SCO properties are consi-derably different[11,13]. While compound **1** has an abrupt spin transition with a thermal hysteresis loop, [Fe^{Ⅲ}(Him)$_2$(4-MeOhapen)]·PF$_6$ showed a gradual spin equilibrium between the HS and LS states; and [Fe^{Ⅲ}(Him)$_2$(4-MeOhapen)]·CF$_3$SO$_3$ showed a spin-transition between 4HS and HS-HS-HS-LS states. They also have different transition temperatures. These differences should be originated from the different

counter anions (CH$_3$SO$_3^-$, CF$_3$SO$_3^-$ and PF$_6^-$) and the resulted H-bond patterns. Although all three compounds have similar chain structures constructed by H-bonds between the anions and axial imidazole molecules, the H-bond strengths and patterns are different between compound **1** and the other two compounds. The N⋯O distances in **1** are shorter compared to the N⋯O distances in [Fe^{III}(Him)$_2$(4-MeOhapen)]·CF$_3$SO$_3$ and N⋯F distances in [Fe^{III}(Him)$_2$(4-MeOhapen)]·PF$_6$ just as anticipated (Table 4). More importantly, in **1**, the H-bond between the imidazole and CH$_3$SO$_3^-$ anion along the chain has a much shorter [N−H⋯O⋯H−N] bridging pattern, while in the other two compounds, the H-bonds have longer patterns: [N−H⋯O−S−O⋯H−N] with CF$_3$SO$_3^-$ anion and [N−H⋯F−P−F⋯H−N] with PF$_6^-$ anion. The shorter bridging pattern in **1** involving only one O atom is more rigid and more efficient to transfer the elastic interactions between the two [Fe^{III}(Him)$_2$(4-MeOhapen)]$^+$ cations. We believe this is responsible for the higher cooperativity in **1**.

Table 4 Hydrogen bond distances (nm) in [Fe^{III}(Him)$_2$(4-MeOhapen)]·CF$_3$SO$_3$ and [Fe^{III}(Him)$_2$(4-MeOhapen)]·PF$_6$

[Fe^{III}(Him)$_2$(4-MeOhapen)]·CF$_3$SO$_3$ (150 K)*			
A	B	C	D
N(4)⋯O(5) 0.271 8(15)	0.280 8(14)	0.282 7(15)	0.280 8(14)
N(6)⋯O(7) 0.290 3(14)	0.287 8(14)	0.287 3(14)	0.289 1(14)
[Fe^{III}(Him)$_2$(4-MeOhapen)]·PF$_6$ (170 K)			
N(4)⋯F(1)	0.292 1(6)		
N(6)⋯F(3)	0.304 7(6)		

* There are four unique CF$_3$SO$_3^-$ anions in the structure of the compound at 150 K.

3　Conclusions

In summary, we have successfully synthesized and characterized one new Fe(Ⅲ) SCO compound based on a tetradentate Schiff base ligand. Hydrogen-bonded chain structure was formed by the hydrogen bonds between the cations and the anions. This compound exhibits an abrupt spin transition with a 4 K thermal hysteresis at around 160 K. The hydrogen bonds between the cations and the anions are believed to be responsible for its abrupt SCO transition. New

Fe(Ⅲ) SCO compounds with different organosulfonate anions and hydrogen bonds are pursued in our lab.

References:

[1] Gütlich P, Goodwin H A. *Spin Crossover in Transition Metal Compounds*: *Vol.*1/2/3. Berlin: Springer Verlag, **2004**.

[2] Halcrow M A. *Spin Crossover Materials*: *Properties and Applications*. New York: Wiley, **2013**.

[3] Gatteschi D, Sessoli R, Villain J. *Molecular Nanomagnets*. Oxford, U.K.: Oxford University Press, **2006**.

[4] Woodruff D N, Winpenny R E P, Layfield R A. *Chem. Rev.*, **2013,113**:5110-5148

[5] Li T, Tan G W, Shao D, et al. *J. Am. Chem. Soc.*, **2016,138**: 10092-10095

[6] Fujita W, Awaga K. *Science*, **1999,286**:261-262

[7] Sato O. *Nature Chemistry*, **2016,8**:644-656

[8] Brooker S. *Chem. Soc. Rev.*, **2015,44**:2880-2892

[9] Harding D J, Harding P, Phonsri W. *Coord. Chem. Rev.*, **2016,313**:38-61

[10] Nihei M, Shiga T, Maeda Y, et al. *Coord. Chem. Rev.*, **2007,251**:2606-2621

[11] Miyano K, Nishida T, Ono H, et al. *Inorg. Chim. Acta*, **2016,439**:49-54

[12] Hanahara K, Ono H, Fujinami T, et al. *Inorg. Chim. Acta*, **2015,429**:93-98

[13] Fujinami T, Ikeda M, Koike M, et al. *Inorg. Chim. Acta*, **2015,432**:89-95

[14] Fujinami T, Hamada D, Matsumoto N, et al. *Inorg. Chim. Acta*, **2015,430**:239-244

[15] Fujinami T, Koike M, Matsumoto N, et al. *Inorg. Chem.*, **2014,53**:2254-2259

[16] Koike M, Murakami K, Fujinami T, et al. *Inorg. Chim. Acta*, **2013,399**:185-192

[17] Weber B, Bauer W, Obel J. *Angew. Chem. Int. Ed.*, **2008, 47**:10098-10101

[18] Zhao X H, Zhang S L, Shao D, et al. *Inorg. Chem.*, **2015,54**: 7857-7867

[19] Shen F X, Pi Q, Shi L, et al. *Dalton Trans.*, **2019,48**:8815-8825

[20] *SAINT, Ver.* 7.68*A*, Bruker AXS, Inc., Madison, WI, **2009**.

[21] Sheldrick G M. *SADABS, Ver.*2008/1, Bruker AXS, Inc., Madison, WI, **2008**.

[22] Sheldrick G M. *SHELXTL, Ver.*6.14, Bruker AXS, Inc., Madison, WI, **2000~2003**.

[23] Dolomanov O V, Bourhis L J , Gildea R J, et al. J. *Appl. Crystallogr.*, **2009,42**:339-341

[24] Kennedy B J, McGrath A C, Murray K S, et al. *Inorg. Chem.*, **1987,26**:483-495